European Polymer Journal 87 (2017) 84–98

Contents lists available at ScienceDirect

European Polymer Journal

journal homepage: www.elsevier.com/locate/europolj

Synthesis and characterization of biobased poly(butylene succinate-*ran*-butylene adipate). Analysis of the composition-dependent physicochemical properties

Thibaud Debuissy, Eric Pollet, Luc Avérous *

BioTeam/ICPEES-ECPM, UMR CNRS 7515, Université de Strasbourg, 25 rue Becquerel, 67087 Strasbourg Cedex 2, France

ARTICLE INFO

Article history:
Received 23 November 2016
Received in revised form 8 December 2016
Accepted 12 December 2016
Available online 18 December 2016

Keywords:
Copolyesters synthesis
Structure-properties relationship
Thermal property
Isodimorphism
Thermal stability
Co-crystallization

ABSTRACT

Fully biobased aliphatic random poly(butylene succinate-*ran*-butylene adipate) (PBSA) copolyesters and the corresponding homopolyesters (poly(butylene succinate) (PBS) and poly(butylene adipate) (PBA)) with high molar mass, were synthesized with different succinic acid/adipic acid (SA/AA) molar ratio by transesterification in melt, using titanium (IV) isopropoxide as an effective catalyst. All synthesized copolyesters were fully characterized by various chemical and physicochemical techniques including NMR, SEC, FTIR, WAXS, DSC and TGA. The final copolyesters molar compositions were identical to the feed ones. The different sequences based on succinate and adipate were randomly distributed along the chains. All the corresponding copolyesters showed an excellent thermal stability with a degradation onset temperature higher than 290 °C and a thermal degradation profile driven by the major diacid component. Glass transition temperatures of copolyesters decreased with the adipate content due to the decrease of the chain mobility, following the Gordon-Taylor relation. PBSA showed a pseudo-eutectic melting behavior characteristic of an isodimorphic character. Besides, the presence of both crystalline phases was observed for adipate content in the range 50–60 mol.%.

1. Introduction

Over the last decades, renewable polymers from biomass have attracted considerable attention, as a sustainable alternative to fossil-based materials. These biobased polymers can bring new macromolecular architectures with the corresponding advanced properties. Among them, poly(lactic acid) [1], poly(butylene succinate) (PBS) [2], poly(hydroxyalkanoates) [3] have seen their interest growing on an industrial point of view with various applications such as packaging, agriculture, sanitary or in biomedical engineering.

The development of biorefinery through the world was a huge step in the production of corresponding biobased monomers or building blocks, such as succinic acid (SA), 1,4-butanediol (1,4-BDO), adipic acid (AA), furans, glycerol and others [4,5]. SA is a well-known short dicarboxylic acid, listed by the US-DoE as one of the strategic platform chemicals from renewable resources [5–8]. Biobased SA is commercialized by different companies (*e.g.*, BioAmber, Myriant, Succinity and Reverdia) and has seen its interest also growing for the production of polyesters (*e.g.*, PBS), polyamides... [5,7] 1,4-BDO is a short diol mainly obtained *via* a chemical process of hydrogenation from SA [4,7,8]. However, recently Genomatica has genetically

* Corresponding author.
E-mail address: luc.averous@unistra.fr (L. Avérous).

http://dx.doi.org/10.1016/j.eurpolymj.2016.12.012
0014-3057/

modified *E. Coli* for the direct bioproduction of 1,4-BDO from sugars [9]. Produced at an industrial level by different companies (Novamont, BioAmber, Genomatica-BASF), biobased 1,4-BDO is largely used, for instance, as chain extender in the polyurethane synthesis [10,11] or as building block for the synthesis of various polyesters and polyamides [12]. AA is a very interesting aliphatic six-carbon diacid also used as building block in the synthesis of polyamides, polyurethanes and polyesters [12,13]. Recently, new biological pathways were discovered for the bioproduction of AA from different biomass such as glucose [14], lignin [15] and fatty acids [16].

Biobased aliphatic polyesters have attracted increasing interest mainly since around two decades. They have been studied from both academic and industrial perspectives, due to their excellent properties and also very often, biodegradability. PBS is one of the most interesting aliphatic polyesters due to its very high melting point, excellent mechanical properties close to some polyolefins [17], biodegradability and easy processability. From the different chemical structures and the large availability of biobased building blocks, various other polyesters can be obtained such as poly(butylene adipate) (PBA) which has a lower melting point and is more readily biodegraded than PBS [17]. As a route to develop materials with improved properties, tailor-made aliphatic copolyesters were synthesized combining different biobased building blocks. Biodegradable aliphatic polyesters such as PBS and poly(butylene succinate-co-butylene adipate) (PBSA) copolymer have been developed at an industrial level since 1990 by Showa Denko (Japan) under tradename "Bionolle". PBSA copolyester has an excellent processability [18] and also present lower melting temperature, lower degree of crystallinity and higher biodegradability than PBS [19].

Through the literature, different PBSA copolyesters with various compositions have been synthesized either by polycondensation from 1,4-BDO and diacids (SA and AA) [20] or by transesterification from 1,4-BDO and dimethyl esters of SA and AA [21–23]. The influence of the PBSA composition on its physical, thermal, mechanical and biodegradation properties was investigated [20–23]. Nevertheless, different parameters and properties such the sequence distribution, the thermal degradation, the isodimorphism and the co-crystallization of PBSA were not studied in details in these previous works, which were more particularly focused on degradation or biodegradation analysis by hydrolytic [20] or enzymatic ways [21–24] in different media such as soil [22], landfill [20]. . . .

To synthesize high molar mass aliphatic polyesters from diacid and diol buildings blocks, the transesterification polycondensation reaction from the melt with an organometallic catalyst is the most used and promising way [12,20]. Moreover, the literature shows that titanium-based catalysts are the most efficient organometallic catalysts for the transesterification reaction, compared to other zirconium, tin, hafnium or antinomy-based catalysts [25].

The aim of this study was, thus, to synthesize and characterize high molar mass PBSA copolyesters and the corresponding homopolyesters (PBS and PBA. They were produced by transesterification polycondensation reaction in melt, with a titanium-based organometallic catalyst, and with different SA/AA ratios. Chemical and physicochemical properties of these different macromolecular architectures were fully investigated by ^{1}H, ^{13}C, ^{31}P NMR, SEC and FTIR. The thermal stability, crystalline structure and thermal properties were analyzed by TGA, WAXS and DSC, respectively. The effect of the SA/AA molar composition on the physicochemical properties was particularly discussed.

2. Experimental part

2.1. Materials

Biobased succinic acid (SA) (99.5%) was kindly supplied by BioAmber (France). SA was bioproduced by fermentation of glucose (from wheat or corn) and obtained after a multistep process based on several purifications, evaporation and crystallization stages. 1,4-butanediol (1,4-BDO) (99%), methanol ($\geqslant$99.6%), chloroform (99.0–99.4%), chromium (III) acetyl acetonate (97%), tetramethyl-1,3,2-dioxaphospholane (Cl-TMDP, 95%) and cholesterol (>99%) were purchased from Sigma-Aldrich. Pyridine HPLC grade (99.5 + %) was purchased from Alfa Aesar. Adipic acid (AA) (99%), titanium (IV) isopropoxide (TTIP) (98 + %) and extra dry toluene (99.85%) were supplied by Acros. All reactants were used without further purification. All solvents used for the analytical methods were of analytical grade.

2.2. Synthesis of copolyesters

Different aliphatic copolyesters were synthesized by a two-stage melt polycondensation method (esterification and transesterification). Syntheses were performed in a 50 mL round bottom flask with a distillation device in order to remove all the by-products from the reaction (mostly water). All reactions were carried out with a diol (1,4-BDO)/acid (SA and/or AA) molar ratio of 1.1/1.

During the first step (esterification), the reaction mixture was maintained under a constant argon flux and magnetically stirred at 300 rpm. The temperature of the reactor was set to 210 °C for 3 h. After 3 h of oligomerization, the remaining by-product of the reaction was distilled off by reducing the pressure to 200 mbar for 5 min, and then the proper amount (0.1 mol.% *vs.* the respective amount of diacid) of a 5 wt.% solution of TTIP in extra dry toluene was introduced inside the reactor. The reaction mixture was stirred at the same temperature as before under a constant argon flux for 45 min. In a second step (transesterification), the temperature of the reactor was slowly increased to 230 °C and the pressure was decreased stepwise over periods of 5 min at 100, 50 and 25 mbar, respectively, in order to avoid excessive foaming and to minimize

oligomer sublimation, which is a potential issue during the melt polycondensation. Finally, the pressure was decreased to 1–3 mbar and the transesterification continued for about 3–4 h. The global reaction scheme and conditions involved are summarized in Scheme 1. At the end, the synthesized polyester had a slightly yellowish color. The reaction mixture was cooled down, dissolved in chloroform, precipitated into a large volume of vigorously stirred dry ice-cold methanol. Thereafter, the precipitate was filtered with a fine (0.45 μm) filter, washed with cold methanol and dried under reduced pressure in an oven at 40 °C for 24 h. Ivory white solid polyesters were finally recovered.

Several poly(butylene succinate-*co*-butylene adipate) (PBSA) copolyesters were synthesized with different SA/AA molar ratios (100/0, 80/20, 60/40, 50/50, 40/60, 20/80 and 0/100). Samples are named "PBSxAy" with x and y as the molar proportion of succinate and adipate determined by ^{1}H NMR, respectively. The two homopolyesters ($PBS_{100}A_0$ and PBS_0A_{100}) are also named as PBS and PBA, respectively.

2.3. General methods and analysis

^{1}H and ^{13}C NMR spectra of polyesters were obtained on a Bruker 400 MHz spectrometer. $CDCl_3$ was used as solvent to prepare solutions with concentrations of 8–10 and 30–50 mg/mL for ^{1}H NMR and ^{13}C NMR, respectively. The number of scans was set to 128 for ^{1}H NMR and at least 5000 for ^{13}C NMR. Calibration of the spectra was performed using the $CDCl_3$ peak (δ_H = 7.26 ppm, δ_C = 77.16 ppm).

^{31}P NMR was performed after phosphitylation of the samples, according to standard protocols [26]. An accurately weighed amount of sample (approx. 100 mg) was dissolved in 500 μL of anhydrous $CDCl_3$. 100 μL of a standard solution of cholesterol (0.1 M in an anhydrous $CDCl_3$/pyridine (1/1.6) solution) containing Cr(III) acetyl acetonate as relaxation agent was then added. Finally, 50 μL of 2-chloro-4,4,5,5-tetramethyl-1,3,2-dioxaphospholane (Cl-TMDP) were added and the mixture was stirred at room temperature for 2 h. Spectra were recorded on a Bruker 400 MHz spectrometer (256 scans at 20 °C). All chemical shifts reported are relative to the reaction product of water with Cl-TMDP, which gives a sharp signal in pyridine/$CDCl_3$ at 132.2 ppm. The quantitative analysis of end-groups and the calculation of molar masses by ^{31}P NMR were performed based on previous reports [26,27].

Size exclusion chromatography (SEC) was performed to determine the number-average molar mass (M_n), the mass-average molar mass (M_w) and the dispersity (Đ) of the samples. A Shimadzu liquid chromatograph was equipped with PLGel Mixed-C and PLGeL 100 Å columns and a refractive index detector. Chloroform was used as eluent at a flow rate of 0.8 ml/min. The instrument was calibrated with linear polystyrene standards from 162 to 1,650,000 g/mol.

Infrared spectroscopy (IR) was performed with a Nicolet 380 Fourier transformed infrared spectrometer (Thermo Electron Corporation) used in reflection mode and equipped with an ATR diamond module (FTIR-ATR). The FTIR-ATR spectra were collected at a resolution of 4 cm^{-1} and with 64 scans per run.

Differential scanning calorimetry (DSC) was performed using a TA Instrument Q 200 under nitrogen (flow rate of 50 mL/min), calibrated with high purity standards. Samples of 2–3 mg were sealed in aluminum pans. A three-step procedure with a 10 °C/min ramp was applied that involved: (1) heating up from room temperature to 130 °C and holding for 3 min to erase the thermal history, (2) cooling down to −80 °C and holding for 3 min and (3) heating (second heating) from −80 °C to 130 °C. To determine the glass transition temperature (T_g), (co)polyesters samples in pans were melted at 130 °C, quickly quenched in liquid nitrogen in order to obtain fully amorphous (co)polyesters and then heated from -80 to 0 °C at 10 °C/min. The degree of crystallinity (X_c) of (co)polyesters was calculated according to Eq. (1),

$$X_c\ (\%) = \frac{\Delta H_m}{\Delta H_m^0} \times 100 \tag{1}$$

where the melting enthalpy (ΔH_m) is taken from the first heating run and ΔH_m^0 is the melting enthalpy of a 100% pure crystalline polyester.

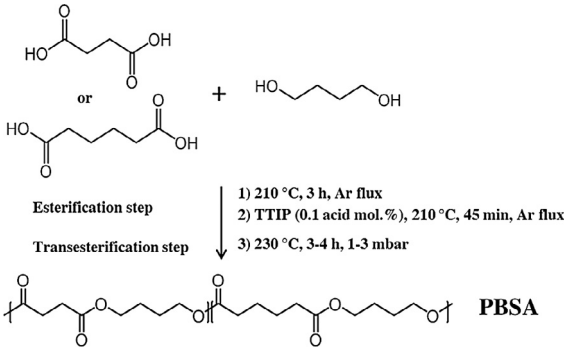

Scheme 1. Reaction procedure for PBSA organometallic synthesis.

Thermal degradations were studied by thermogravimetric analyses (TGA). Measurements were conducted under helium atmosphere (flow rate of 25 mL/min) using a Hi-Res TGA Q5000 apparatus from TA Instruments. Samples (1–3 mg) were heated from room temperature up to 600 °C at a rate of 20 °C/min.

Wide angle X-ray Scattering (WAXS) data were recorded on a Siemens D5000 diffractometer (Germany) using Cu K_α radiation (1.5406 Å) at 25–30 °C in the range of $2\theta = 14–32°$ at 0.4° min^{-1}. Analyses are performed on compression-molded sheets.

2.4. Ester function density

The ester function density of polyesters is defined by the number of ester function by repetitive unit on the number of carbons in the main chain by repetitive unit. The ester function density of PBSA copolyesters ($D_{ester,PBSA}$) is defined by Eq. (2),

$$D_{ester,PBSA} = \chi_{SA} \times D_{ester,PBS} + \chi_{AA} \times D_{ester,PBA} \quad (2)$$

where χ_{SA} and χ_{AA} are the succinate and adipate contents in copolyester, respectively; $D_{ester,PBS}$ and $D_{ester,PBA}$ are ester function densities of PBS and PBA, respectively.

3. Results and discussion

3.1. Characterization of macromolecular architectures of synthesized copolyesters

Different PBSA copolyesters were produced by a two-step melt polycondensation method (Scheme 1). In the first step, the non-catalyzed esterification reaction between 1,4-BDO and a mixture of diacid (SA/AA) resulted in formation of oligomers, which reached M_n of about 2000–3000 g/mol (determined by SEC) after 3 h of esterification, necessary to avoid any removal phenomenon (*e.g.* monomer sublimation) during the next step. Then, TTIP was added into the reaction mixture and the transesterification, under vacuum, of the previously synthesized oligomers resulted in a significant increase of copolyesters molar masses. The corresponding molar masses are presented in Table 1. The synthesized copolyesters could be considered as high molar mass polyesters since the samples have M_n higher than 27,000 g/mol, with a dispersity (Đ) of about 1.4–1.9. Đ were slightly lower than the expected value of 2, especially for the 20/80 (SA/AA) composition. One can suppose a small loss of the shortest oligomers during the dissolution/precipitation process even if maximum care (small filter, dry ice cold methanol) was taken to recover the maximum amount of product. Polymerization yields determined after precipitation of samples were rather high and only varied in a narrow range (approx. 85–90%).

The final (co)polyester chemical structures were analyzed by ^1H, ^{13}C, ^{31}P NMR and FTIR. ^1H NMR results are presented in Fig. 1a, and in SI.1 from Supporting Information (SI), respectively. In ^1H NMR spectra, the presence of ester functions was verified by the signal at $\delta = 4.10$ ppm assigned to COO-C$\underline{H_2}$-CH_2-protons from 1,4-BDO repeating units. This signal is complex due to the influence of neighboring dicarboxylate units (*i.e.* two triplets at 4.11 and 4.09 ppm were detected for the neighboring succinate (SA) and adipate (AA) units, respectively). ^1H chemical shifts at $\delta = 1.65$, 1.70, 2.32 and 2.62 ppm were ascribed to CO—CH_2—C$\underline{H_2}$-protons from AA repeating units, to O—CH_2—C$\underline{H_2}$-protons from 1,4-BDO repeating units, to CO—C$\underline{H_2}$—CH_2-protons from AA repeating units and to CO—C$\underline{H_2}$-protons from SA repeating units, respectively. Interestingly, the hydroxyl terminal group (HO—C$\underline{H_2}$—) signal was detected at $\delta = 3.67$ ppm, with low intensities, in agreement with the relatively high molar mass of the samples. The succinate (χ_{SA}) and adipate (χ_{AA}) contents of synthesized copolyesters was calculated from ^1H NMR spectra using relative intensities of methylene protons in α of ester functions in succinate ($\delta = 2.62$ ppm) and adipate ($\delta = 2.32$ ppm) segments (more details in SI.2). Determined χ_{SA} and χ_{AA} contents in the chains are given in Table 1. All synthesized copolyesters presented SA/AA molar ratio equivalent to the initial feed ones. The chosen pathway allows to perform an accurate fabrication of copolyesters with a targeted composition. Previous studies showed

Table 1
Molar composition and molar masses of synthesized PBSA copolyesters.

Sample	Feed SA/AA composition mol.%	^1H NMR Determined SA /AA composition mol.%	^1H NMR $M_{n,1H\ NMR}$ kg/mol	SEC $M_{n,SEC}$ kg/mol	SEC Đ	^{31}P NMR $M_{n,31P\ NMR}$ kg/mol	^{31}P NMR OH end-groups %	^{13}C NMR L_{PS}	^{13}C NMR L_{PA}	^{13}C NMR R
PBS ($PBS_{100}A_0$)	100/0	100/0	19.7	39.2	1.7	17.3	78	–	–	–
$PBS_{79}A_{21}$	80/20	79.2/20.8	15.5	39.7	1.9	16.4	65	4.8	1.3	1.00
$PBS_{59}A_{41}$	60/40	58.6/41.4	12.3	26.8	1.8	9.5	41	2.6	1.6	1.01
$PBS_{50}A_{50}$	50/50	49.7/50.3	11.4	44.5	1.6	13.7	60	2.0	2.0	1.00
$PBS_{39}A_{61}$	40/60	39.1/60.9	12.2	41.4	1.6	12.0	55	1.8	2.4	0.99
$PBS_{21}A_{79}$	20/80	20.9/79.1	9.4	27.4	1.4	10.7	94	1.3	4.2	1.04
PBA (PBS_0A_{100})	0/100	0/100	13.7	33.3	1.8	13.6	79	–	–	–

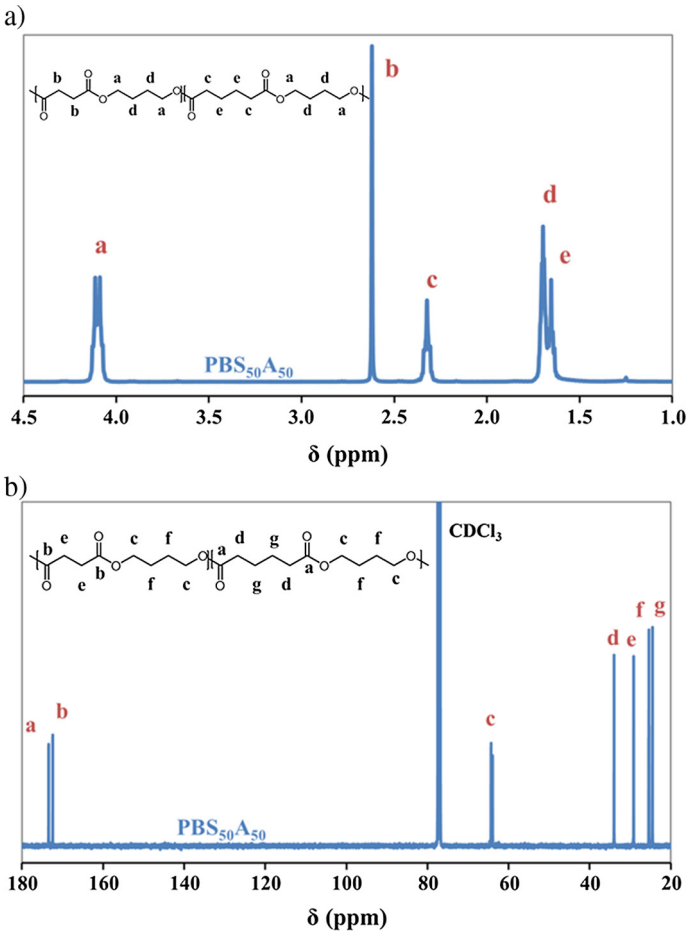

Fig. 1. (a) 1H and (b) ^{13}C NMR of $PBS_{50}A_{50}$ in $CDCl_3$.

that the non-catalyzed esterification rate with AA were much lower than with SA, for small chain length aliphatic diols [28,29]. This can be explained by the small pKa difference of both diacids (*i.e.* $pKa_{,1}/pKa_{,2}$ of 4.16/5.61 and 4.43/5.41 for SA and AA, respectively) which permitted to dissociate an higher proportion of acidic protons inside the reaction mixture, allowing an higher rate of the auto-catalytic reaction. However, the presence of an excess of hydroxyl (OH) functions compared to carboxylic acid (COOH) functions increased the overall esterification rate permitting a higher diacid conversion [30,31]. Moreover, the esterification time was set to 3 h in order to avoid remaining free diacid residual monomers in the system. Finally, these experimental conditions permitted to override the reactivity difference and convert all feed diacid into oligomers before the second reactive step under high vacuum.

To obtain more detailed information about the PBSA architecture, ^{13}C NMR was performed. ^{13}C NMR results are presented in Fig. 1b and in SI.3, respectively. ^{13}C chemical shifts at $\delta = 24.5$, 34.0 and 173.4 ppm were ascribed to CO—CH_2—$\underline{C}H_2$-, CO—$\underline{C}H_2$—CH_2- and $\underline{C}$O—CH_2—CH_2-carbons from AA repeating units, whereas ones at $\delta = 29.1$ and 172.4 ppm were ascribed to CO—$\underline{C}H_2$-and $\underline{C}$O—CH_2-carbons from SA repeating units, respectively. Finally, ^{13}C chemical shifts at $\delta = 25.4$ (three peaks), 64.0 (two peaks) and 64.3 (two peaks) ppm were assigned to O—CH_2—$\underline{C}H_2$-, O—$\underline{C}H_2$—CH_2-next to an adipate repetitive units and O—$\underline{C}H_2$—CH_2-next to a succinate repetitive units, respectively. The sensitivity of the ^{13}C NMR to small differences in the chemical environment enabled us to identify the different triads SBS, SBA, and ABA (with S, B and A standing for SA, 1,4-BDO diol and AA, respectively) presented in Fig. 2a. 1,4-BDO moieties are present in all three triads at distinctly different resonance absorptions close to chemical shifts of PBS ($PBS_{100}A_0$) or PBA (PBS_0A_{100}). Such results, with the splitting of the two signals (carbon atoms a_1, a_2, a_3 and a_4 in Fig. 2), enable the calculation of the average sequence length of BS and BA units (L_{BS} and L_{BA}, respectively) and the degree of randomness (R) using Eqs. (3)–(5),

$$L_{BS} = 1 + \frac{2 \times I_{SBS}}{I_{SBA-S} + I_{SBA-A}} \tag{3}$$

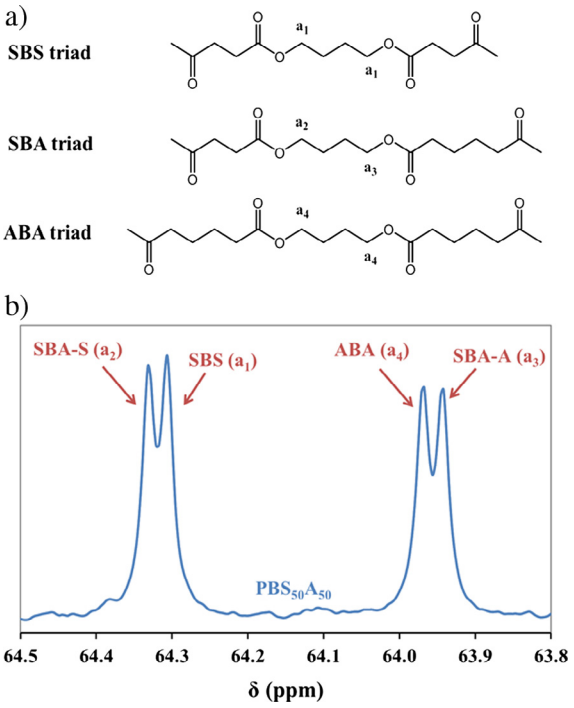

Fig. 2. (a) Possible triads of PBSA copolyesters, (b) ^{13}C NMR spectra of $PBS_{50}A_{50}$ with high number of scans centered at $\delta \sim 64$ ppm.

$$L_{BA} = 1 + \frac{2 \times I_{ABA}}{I_{SBA-S} + I_{SBA-A}} \quad (4)$$

$$R = \frac{1}{L_{BS}} + \frac{1}{L_{BA}} \quad (5)$$

where I_{SBS}, $I_{SBA\text{-}S}$, $I_{SBA\text{-}A}$ and I_{ABA} are intensities of peaks assigned to methylene carbons in α of the ester function in butyl segments ($\delta \sim 64$ ppm) of SBS, SBA-S side, SBA-A side and ABA triads in PBSA copolyesters. The corresponding data are listed in Table 1.

For fully random copolymers, R is equal to 1, whereas it is equal to 2 for strictly alternating, and close to 0 for block copolymers. According to the SA/AA ratio, L_{BS} and L_{BA} varied between 1.3 and 4.8. PBSA copolyesters, composed of both diacids, all showed a randomness degree of about 1.0 meaning a random distribution between succinate and adipate segments along the polyester chain, as it was expected by using titanium-based organometallic catalyst [12,32].

^{31}P NMR analyses were performed in $CDCl_3$ with cholesterol as standard, and presented in Fig. 3a. All copolyesters showed COOH (134.9 ppm) and primary OH (147.4 ppm) end-groups. The majority of the end-groups were OH functions (due to the higher amount of OH initially introduced into the reaction mixture, compared to COOH). However, an important disparity of OH end-groups proportion was determined. Since reported values correspond to one sample by composition and not an average value, results should be considered with care. Moreover, it was interesting to note that SA (134.85 ppm) and AA (134.90 ppm) end-groups were separated in ^{31}P NMR spectra. The proportion of AA end-groups seemed to be slightly superior to the global adipate content into the chain, for almost all copolyesters containing a mixture of diacids (data in SI.4). This latest result was surprising if we take into account the effect of the transesterification, with the corresponding random structure. One can suppose that the difference could come from measurement uncertainty, the small acid signal overlapping (Fig. SI.3) and the possible difference of stability of both acid end-groups with the phosphorus reactant [33].

The calculated M_n of copolyesters by ^{31}P NMR ($M_{n,\ 31P\ NMR}$), reported in Table 1, were approx. 2–3 times smaller compared to the one obtained by SEC, the latter being overestimated partly due to the calibration based on PS standards. M_n determined by ^{31}P NMR varied between 9500 and 17,000 g/mol. This technique gave a more accurate estimation of aliphatic copolyesters molar mass. However, this method based on the quantification of end-groups did not take into account the possible macrocycles that could have been produced during the polyester synthesis, but undetectable by ^{31}P NMR analysis [34,35]. Furthermore, a new method to calculate the molar mass was developed using (i) ^{1}H NMR specific signals of AA, SA, OH end-groups and 1,4-BDO repetitive units at 2.32, 2.62, 3.67 and 4.10 ppm, respectively, and (ii) the OH end-groups proportion determined by ^{31}P NMR. $M_{n,1H\ NMR}$ was calculated according to Eq. (6),

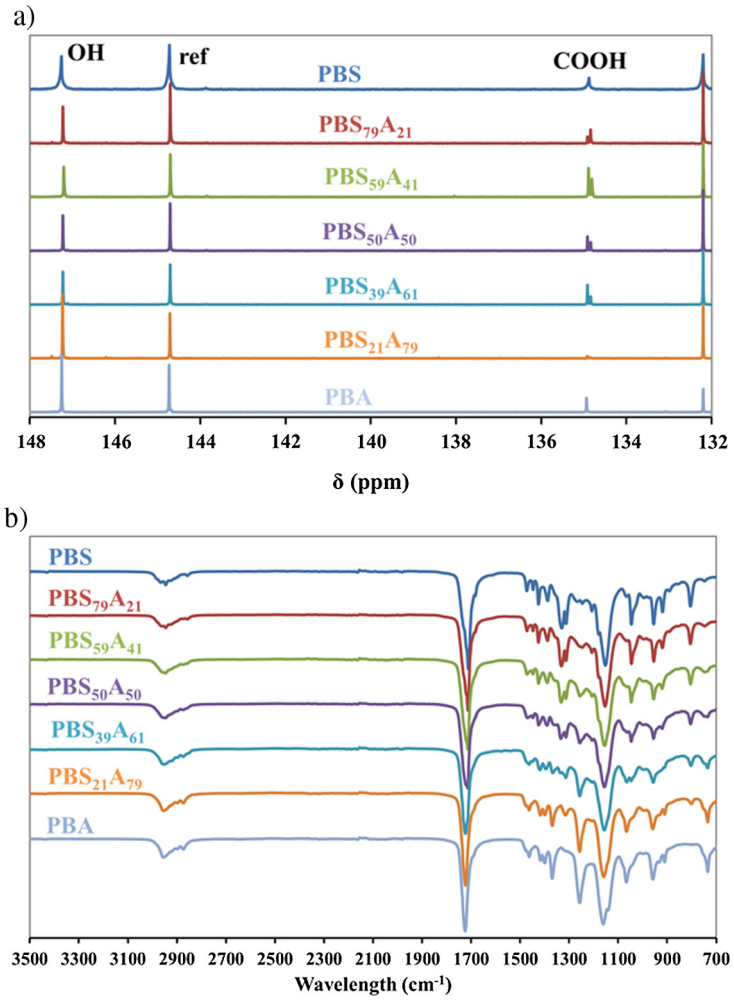

Fig. 3. (a) ^{31}P NMR and (b) FTIR spectra of PBSA copolyesters.

$$M_{n,1H\ NMR} = \frac{\frac{I_{4.12}}{4} \times 88.10 + \chi_{SA} \times \frac{I_{2.62}}{4} \times 84.07 + \chi_{AA} \times \frac{I_{2.32}}{4} \times 112.13 + \frac{I_{3.67}}{2} \times 89.11}{0.5 \times \frac{I_{3.67}}{2}} \times X_{OH} \quad (6)$$

where $I_{4.12}$, $I_{2.62}$, $I_{2.32}$ and $I_{3.67}$ are intensities of 1,4-BDO, SA, AA and OH end-groups respectively; 88.10, 84.07, 112.13 and 89.11 are molar mass of 1,4-BDO, SA, AA and OH end-groups units respectively; χ_{SA} and χ_{AA} are the succinate and adipate contents in copolyester, respectively; X_{OH} is the OH end-groups proportion determined by ^{31}P NMR. $M_{n,1H\ NMR}$ results are reported in Table 1.

Due to the impossibility to quantify COOH end-groups, X_{OH} was used as correcting factor. This method was based on the quantification of OH end-groups and, such as $M_{n,31P\ NMR}$. $M_{n,1H\ NMR}$ of PBSA copolyesters varied between 9500 and 20,000 g/mol. $M_{n,1H\ NMR}$ values were mostly close to the one calculated according to ^{31}P NMR with relative M_n difference, lower than 15%, except for $PBS_{79}A_{21}$ (around 30%).

The FTIR analysis of copolyesters showed some interesting results. FTIR spectra of all copolyesters are presented in Fig. 3b. First, in all copolyesters, no broad signals around 3200–3400 cm^{-1} assigned to the O-H vibration of COOH and OH end-groups were observed due to the high molar mass of the synthesized copolyesters. Then, all samples exhibited a sharp signal at approx. 1710–1725 and 1150–1160 cm^{-1} assigned to the C=O and asymmetric —COO-stretching vibration from ester groups confirming the synthesis of esters functions, respectively. One can observe that the C=O stretching ester vibration slightly shifted from 1710 to 1725 for PBS (or $PBS_{100}A_0$) to PBA (or PBS_0A_{100}), respectively. Moreover signals at 2850–3000 cm^{-1} were assigned to C—H stretching vibrations of methylene carbons. Finally, signals at 1330, 1045 and 805 cm^{-1} assigned to the symmetric C—O stretching, O—CH_2-stretching and —CH_2-rocking vibrations shifted to 1255, 1055 and 735 cm^{-1} with the increase of the adipate content in copolyesters, respectively. There was, thus, a modification of the FTIR spectra profile with the SA/AA composition.

3.2. Thermal degradation

TGA traces of PBSA samples are shown in Fig. 4 with their corresponding derivatives curves (DTG). Data are summarized in Table 2. Under helium, all copolyesters degraded into two main steps which involve competitive mechanisms. First, a small mass loss was observed at 260–315 °C due to the degradation of low molar mass chains along with the cyclization at the chain-ends and back-biting reactions that are responsible for CO_2 and H_2O release, which are produced from the decomposition of COOH and OH chain-ends, respectively (Scheme SI.1) [36,37]. Secondly, a major degradation occurred at 315–425 °C with a substantial mass loss of approx. 90% corresponding to the thermal degradation of polyesters chains, mostly by β- and α-hydrogen bond scissions (Scheme SI.1). These reactions are responsible for the decomposition of polyesters into small compounds such as diacids, vinyl compounds, aldehydes and anhydrides [37,38]. After this decomposition step, mass residue of approx. 4% still remained. This multi-steps degradation is in agreement with previous reports [12,39].

The 2% mass degradation temperature ($T_{d,2\%}$) of all copolyesters were about 290–315 °C. By taking $T_{d,2\%}$ as criterion for the thermal stability of polyesters, PBS possessed the lowest thermal stability, whereas PBA showed the highest one. The 50% mass loss degradation temperature ($T_{d,50\%}$) and the maximal degradation temperature ($T_{deg,max}$) were approx. 365–385 and 375–400 °C, respectively, and both decreased with the adipate content.

Results showed that it seemed appropriate to class copolyesters into two groups according to their composition. PBSA with adipate content of 60 mol.% or higher exhibited a $T_{d,50\%}$ and $T_{deg,max}$ of approx. 370 and 375 °C, whereas PBSA with adipate content lower than 60 mol.% exhibited a $T_{d,50\%}$ and $T_{deg,max}$ of approx. 380–385 and 395 °C, respectively. The thermal degradation profile of "adipate rich" copolyesters was, thus, sharper compared to "succinate rich" copolyesters. DTG curves of $PBS_{79}A_{21}$, $PBS_{59}A_{41}$ and $PBS_{50}A_{50}$ exhibited first a shoulder at approx. 350–360 °C assigned to the degradation of adipate units and, then the degradation assigned to succinate units at 380–400 °C. In conclusion, the thermal degradation profile of PBSA depended highly on the SA/AA molar ratio. This result was in contradiction with a previous study which showed that the degradation mechanism depended highly on the type of diol unit, whereas the influence of the carboxylic acid unit was less important [40]. Therefore, since the same diol was used in this study, its influence on the degradation was not investigated and, thus, the influence on the diol *vs.* the influence of the diacid was not possible. Nevertheless, the present results proved that the influence of the diacid was not negligible.

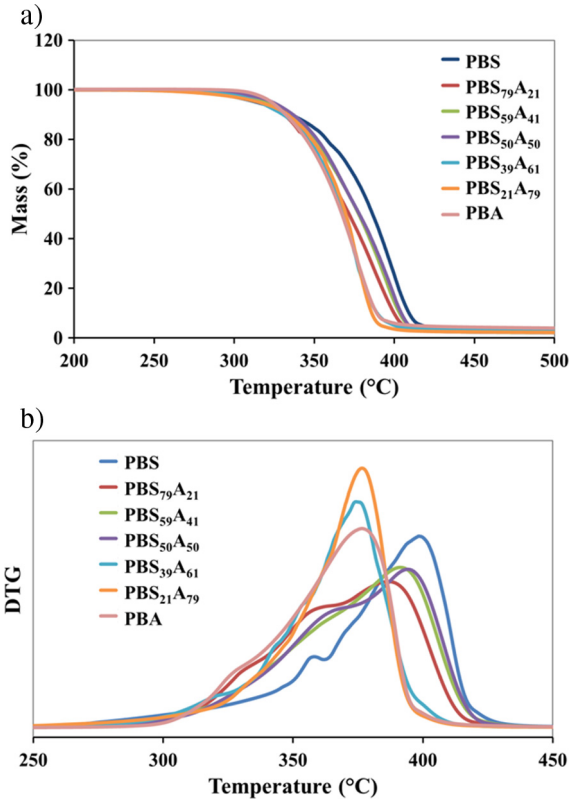

Fig. 4. (a) Mass loss and (b) DTG curves of PBS, PBSA copolyesters and PBA under helium at 20 °C/min.

Table 2
TGA results of PBSA copolyesters in helium with a heating rate of 20 °C/min.

Sample	D_{ester} %	$T_{d,2\%}$ °C	$T_{d,50\%}$ °C	$T_{deg,max}$ °C	Residue at 500 °C wt.%
$PBS_{100}A_0$ (PBS)	25.0	293	386	398	2.7
$PBS_{79}A_{21}$	24.0	302	371	387	2.8
$PBS_{59}A_{41}$	23.0	300	378	394	2.2
$PBS_{50}A_{50}$	22.5	308	378	397	2.2
$PBS_{39}A_{61}$	22.0	297	368	374	3.2
$PBS_{21}A_{79}$	21.0	294	370	376	2.2
PBS_0A_{100} (PBA)	20.0	314	367	377	4.0

3.3. WAXS and DSC results

To investigate the crystalline structure of copolyesters, a WAXS study was first performed. The patterns of PBSA copolyesters are shown in Fig. 5. WAXS patterns of the copolyesters appeared to be characterized by well-defined diffraction peaks over the whole composition range. The patterns of semi-crystalline copolyesters could be divided into three groups according to the adipate content: copolyesters containing 50 mol.% or less of adipate units are characterized by X-ray patterns very similar to PBS, indicating that the crystal structure in these copolyesters has the same characteristics as the PBS lattice. On the contrary, samples containing >61 mol.% of adipate units crystallized according to the PBA lattice. Finally, it was interesting to note that $PBS_{39}A_{61}$ seemed to exhibit both crystalline phases.

The crystal structure of PBS was in agreement with previous reports and defined in α-form characterized by monoclinic unit cell [41]. The reflections for PBS appeared at 2θ = 19.4, 21.7, 22.4 and 28.7°. The crystal structure of PBA has been already studied [41]. Two crystalline forms were identified such as (i) the α-form which is characterized by a monoclinic unit cell, mainly formed at low cooling rate (thermodynamically favored) and high temperature of crystallization (T_c) (>32 °C), and (ii) the β-form which is characterized by chains in a planar zigzag conformation packed in a orthorhombic unit cell, formed at high cooling rate (kinetically favored) and low T_c (< 28 °C). Our sample of PBA exhibited reflections at 2θ = 21.3 and 24.4° assigned to β-form crystals, but also reflections at 2θ = 21.6, 22.3 and 24.1° assigned to α-form crystals. PBS exhibited thus α + β mixed crystals [42].

$PBS_{79}A_{21}$, $PBS_{59}A_{41}$, $PBS_{50}A_{50}$ and $PBS_{39}A_{61}$ showed diffraction patterns similar to PBS, but with lower intensities. The co-monomeric unit (adipate in this case) incorporated in minor amount was found to be excluded from the PBS crystal lattice or only partially integrated in it. This phenomenon decreased the crystal strength and lamellae sizes due to the presence of "adipate defects" inside the chain and, thus, the degree of crystallinity decreased with the adipate content. The presence of defects in the chain led to a small modification of the crystalline structure proved by the quite larger and slightly shifted copolyesters diffraction peaks compared to those of homopolyesters. Contrary to PBA, $PBS_{21}A_{79}$ and $PBS_{39}A_{61}$ seemed to show only β-form crystals of PBA. One can suppose that this could be due to the inclusion of succinate units inside the PBA crystalline phase which disrupted the homogeneity of the polyester chain, slowed down the crystallization rate and, thus, only kinetically-favored β-form crystals of PBA were formed during the crystallization of $PBS_{21}A_{79}$ and $PBS_{39}A_{61}$. Finally, in $PBS_{39}A_{61}$, the β-form PBA crystalline phase was dominant but a small PBS crystalline phase was also present in the sample. The presence of both crystalline phases could be explained by the close unit cells and structures of PBS and PBA, and by the high amount of both segments at this composition.

In complement to WAXS analysis, the degree of crystallinity and thermal properties of copolyesters were studied by DSC. Prior to this, it has been verified, from TGA results, that no significant degradation occurred on the samples in the DSC analyses temperature range. Cooling and second heating run curves are presented in Fig. 6 and all corresponding data are summarized in Table 3. Fig. 7-a plotted the crystallization temperatures (T_c) and enthalpies (ΔH_c) of (co)polyesters, measured during the cooling run, as a function of the adipate content, whereas Fig. 7b plotted T_g of (co)polyesters as a function of the adipate content. The melting temperatures (T_m) and enthalpies (ΔH_m) of (co)polyesters, measured during the second heating run, as a function of the adipate content are plotted in Fig. 8. The variation of thermal properties is also discussed as a function of D_{ester}, calculated according to Eq. (2).

At the beginning, all (co)polyesters were melted in order to erase the thermal history. During the cooling run from the melt at controlled speed (10 °C/min), all samples showed an exothermic phenomenon attributed to the crystallization. T_c decreased with the adipate content from 83 °C for PBS until reaching a minimal T_c of −16 °C for $PBS_{50}A_{50}$. Then, T_c increased again to reach 32 °C for PBA. Fig. 7a exhibited, thus, a pseudo-eutectic behavior for T_c, but also another pseudo-eutectic behavior for ΔH_c with a minimal value for the $PBS_{39}A_{61}$ copolyester. The addition of a co-monomeric unit in the homopolyester matrix disrupted the structure and, thus, decreased the lamellae size and crystal strength. Moreover, crystallization peaks became larger with the increase of the co-monomeric unit content in the homopolyester, which reduced the crystal homogeneity as observed in WAXS.

The second heating run was characterized by a small endothermal baseline deviation associated to the glass-transition phenomenon and an endothermic peak at higher temperature, associated to a melting phenomenon. Moreover, $PBS_{59}A_{41}$ exhibited, in addition to these two phenomena, an exothermic signal attributed to a cold-crystallization at approx.

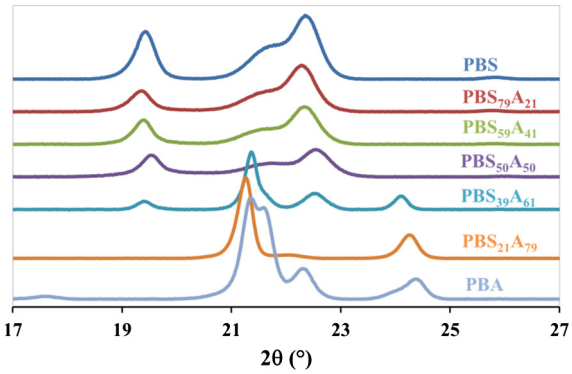

Fig. 5. WAXS patterns of PBS, PBSA copolyesters and PBA.

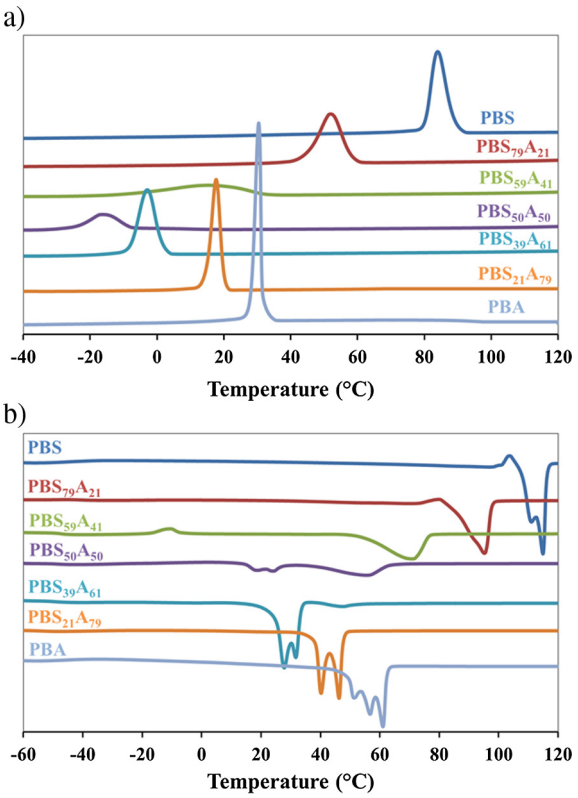

Fig. 6. (a) Cooling and (b) second heating run curves of PBS, PBSA copolyesters and PBA at 10 °C/min.

Table 3
DSC results of PBSA copolyesters with heating and cooling rate of 10 °C/min.

Sample	D_{ester} %	First heating			Cooling			Second heating				
		T_m °C	ΔH_m J/g	X_c %	T_c °C	ΔH_c J/g	T_g[a] °C	T_{cc} °C	ΔH_{cc} J/g	T_m °C	ΔH_m J/g	X_c %
PBS ($PBS_{100}A_0$)	25.0	116	81	39	83	67	−37	–	–	115	65	31
$PBS_{79}A_{21}$	24.0	95	47	22	52	49	−44	–	–	95	46	22
$PBS_{59}A_{41}$	23.0	72	42	20	15	31	−48	−11	4	71	37	18
$PBS_{50}A_{50}$	22.5	51	41	20	−16	32	−51	–	–	24/56[b]	10/26[b]	7/12[b]
$PBS_{39}A_{61}$	22.0	43	26	19	−3	42	−53	–	–	32/47[b]	44/3[b]	33/2[b]
$PBS_{21}A_{79}$	21.0	49	66	49	18	54	−57	–	–	46	54	40
PBA (PBS_0A_{100})	20.0	58	80	59	32	55	−60	–		57	53	39

[a] T_g values were determined after a quenching from the melt.
[b] Presence of two crystalline phases (PBA phase/PBS phase).

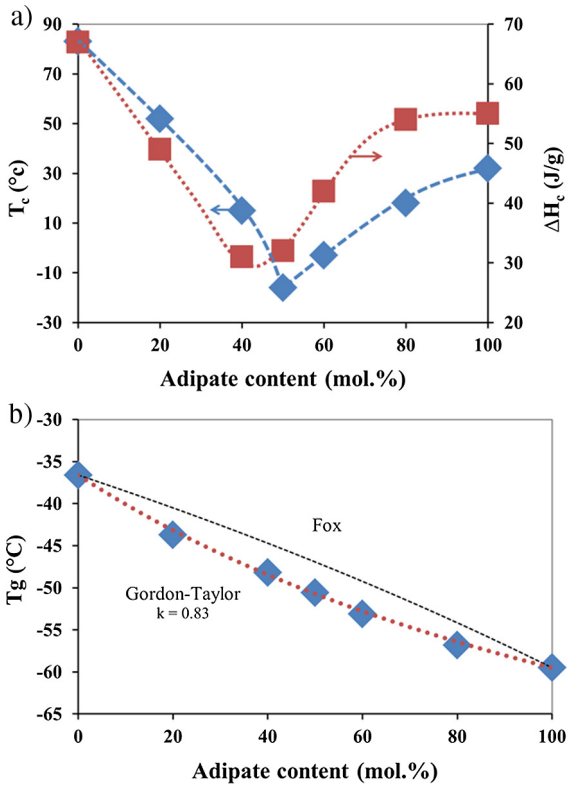

Fig. 7. (a) Variation of T_c and ΔH_c of copolyesters *vs.* adipate content and (b) variation of T_g *vs.* adipate content in PBSA.

−11 °C. The presence of the cold-crystallization phenomena was due to an incomplete crystallization during the cooling run. One can conclude that $PBS_{59}A_{41}$ had, thus, the lowest crystallization rate.

T_g values are summarized in Table 3 and are plotted in Fig. 7b as a function of the adipate content. As can be seen, T_g was influenced by the amount of adipate unit in the copolyester chain. T_g decreased continuously from −37 to −60 °C for adipate content of 0 and 100%, respectively. Indeed, by increasing the amount of adipate unit in the copolyester, D_{ester} decreased. Moreover, it is well known that the second-order transition temperature is considered as a measure of the chain flexibility of the polymer chain. The more flexible the chains are, the lower the T_g is. By decreasing D_{ester} of the copolyester chain, a lower amount of intra or inter-chain interactions between ester groups were possible, whence the decrease of chain mobility leading to the decrease of T_g.

In random copolyesters, T_g is usually a monotonic function of composition. The most common relationship used to predict T_g as a function of a co-monomer content is the Fox equation [43], defined by Eq. (7),

$$\frac{1}{T_{g,copo}} = \frac{w_1}{T_{g,1}} + \frac{w_2}{T_{g,2}} \tag{7}$$

where $T_{g,1}$ and $T_{g,2}$ are the glass transition temperature of pure homopolyesters, and w_1 and w_2 respective mass fractions.

However, as one can observe in Fig. 7b, the Fox equation did not fit at all the experimental data. Thus, an alternative relationship has been considered for copolymers by using a mixing law, the Gordon-Taylor equation [44], defined by Eq. (8),

$$T_{g,copo} = \frac{w_1 T_{g,1} + k(1-w_1) T_{g,2}}{w_1 + k(1-w_1)} \tag{8}$$

where $T_{g,1}$ and $T_{g,2}$ are the glass transition temperature of pure homopolyesters, w_1 the respective mass fraction of the pure homopolyester 1 and k the Gordon-Taylor parameter.

As shown in Fig. 7b, the Gordon-Taylor equation fitted well the experimental data with k = 0.83. In the original version of volume additivity, the parameter $k = \rho_1\Delta\alpha_2/\rho_2\Delta\alpha_1$ has a well-defined significance (ρ_i is the density and $\Delta\alpha_i = \alpha_{melt} - \alpha_{glass}$ is the increment at T_g of the expansion coefficient of the respective component i). But generally k is considered a real fitting parameter [45]. T_g of the copolyesters could be, thus, predicted for all the composition range using this relation.

Fig. 6b highlighted that PBS had the highest T_m at approx. 115 °C. In detail, one can observe that the melting phenomena spread on a large temperature range (100–120 °C) and was composed of two peaks. Moreover, a small cold-crystallization signal was observed just before the melting. These multiple peaks were attributed to the crystallite reorganization during

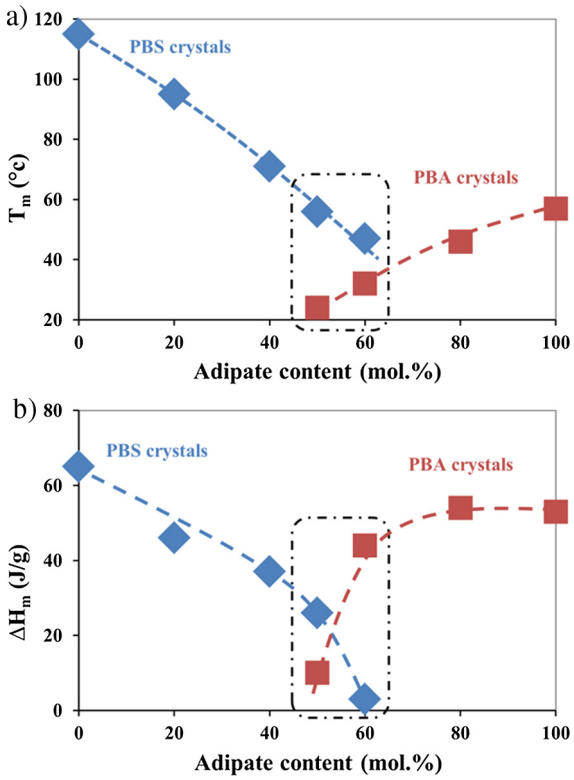

Fig. 8. Variation of (a) T_m and (a) ΔH_m of copolyesters during the second heating run vs. the adipate content.

the heating by a fusion-recrystallization phenomenon [12,21,46]. Such as PBS, PBA melting area spread on a large temperature range (45–65 °C) with three endothermic peaks. They were due, such as PBS, to the fusion-recrystallization phenomenon, but also to the polymorphism of PBA [41]. The copolyesters showed also fusion-recrystallization phenomena. During the second heating run, $PBS_{50}A_{50}$ exhibited two melting phenomena at approx. 24 and 56 °C even if only one crystallization signal was observed during the cooling run. One can suppose the presence of two crystalline phases (*i.e.* PBS and PBA), even if the presence of PBA crystals was not highlighted by WAXS. Nevertheless, WAXS analysis was performed on compressed-molded samples which were quenched during the process and not slowly cooled at 10 °C/min. This can explain the difference of the crystalline structure. Likewise, $PBS_{39}A_{61}$ showed first an intense melting phenomenon at 20–35 °C assigned to the fusion of PBA crystals, followed by a small fusion at approx. 45 °C assigned to the fusion of PBS crystals observed in WAXS.

Fig. 8 showed that T_m and ΔH_m of PBS crystals decreased with the adipate content until $PBS_{39}A_{61}$. On the same way, T_m of PBA crystals decreased with the SA content until $PBS_{50}A_{50}$. $PBS_{50}A_{50}$ and $PBS_{39}A_{61}$ showed the presence of both crystalline phases by DSC in our conditions. However, $PBS_{50}A_{50}$ and $PBS_{39}A_{61}$ crystalline phases are mostly based on PBS and PBA crystals, respectively. This result was in agreement with WAXS results. The variations of T_m and ΔH_m with the composition both showed pseudo-eutectic behaviors with minimal values near the 50/50–40/60 (SA/AA) composition. Moreover, the plot of ΔH_m of copolyesters as a function of the adipate content for the sum of both crystalline phases are presented in SI.6 and showed such as before a pseudo-eutectic behavior with minimal values for adipate content of approx. 39–50 mol.%. The presence of both melting and melting enthalpy pseudo-eutectic points and the presence of different crystalline phases according to the molar composition highlighted the isodimorphic co-crystallization behavior of PBSA as observed for other aliphatic random copolyesters [47,48].

The melting enthalpy value of 100% crystalline phase (ΔH_m°) is determined from the groups contribution method as proposed by Van Krevelen [49] for PBA (135 J/g), and from experimental data [50] for PBS (210 J/g). WAXS results showed that most samples exhibited only one crystal lattice by sample. The degree of crystallinity (X_c) of copolyesters was calculated from the first and second heating scans and values are summarized in Table 3. X_c was plotted as a function of the adipate content and shown in Fig. 9. X_c of PBA was slightly higher than the one of PBS. One can suppose that the decrease of D_{ester} due to adipate units with more methylene groups bring more flexibility to the chain and thus facility to crystallize contrary to succinate units. However, results should be taken with care since ΔH_m° values of PBA and PBS were theoretically and experimentally calculated, respectively. X_c followed the same trend as the melting and crystallization enthalpies with a global decrease of the copolyester degree of crystallinity with the addition of a co-monomeric unit (reduction of block length

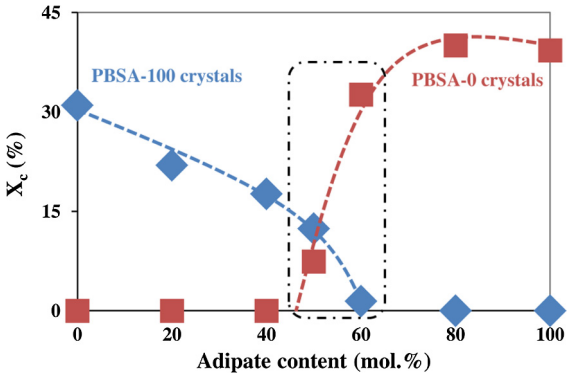

Fig. 9. Degree of crystallinity during the second heating run of PBSA copolyesters in function of adipate content.

inside the chain). However, one can observe that the X_c of $PBS_{21}A_{79}$ during the second heating run is similar (even slightly higher) than the one of PBA. We can suppose that this was more likely due to the lower M_n of $PBS_{21}A_{79}$ than PBA. Nevertheless, during the first heating scan, X_c of $PBS_{21}A_{79}$ was lower than the one of PBA confirming the decrease of the copolyester degree of crystallinity with the addition of a co-monomeric unit.

4. Conclusion

Different biobased copolyesters (PBSA) and homopolymers (PBS and PBA) based on renewable building blocks were successfully synthesized in melt, using TTIP as an effective catalyst, with different compositions. The optimized synthetic pathway permitted to obtain (i) high molar masses, (ii) final copolyesters with the same molar compositions than the initial feed ratios and (iii) a random distribution between succinate and adipate segments along the polyester chain.

PBSA copolyesters exhibited excellent thermal stability until approx. 300 °C. Moreover, the thermal degradation profile of PBSA copolyesters was driven by the major diacid component, resulting in an acceleration of the degradation rate, after the onset, for "adipate rich" copolyesters.

Furthermore, PBSA copolyesters showed an isodimorphic co-crystallization behavior characterized by the presence of one crystalline phase for each sample according to the composition, except for copolyesters with adipate content of 50–60 mol.% which showed the presence of both crystalline phases, and a pseudo-eutectic melting behavior. T_g of copolyesters decreased with the adipate content according to the Gordon-Taylor relation with a calculated Gordon-Taylor parameter, k, of 0.83. The decrease of T_g was ascribed to the increase in copolyester chain mobility resulting from the decrease of the ester function density.

The PBSA copolyester is, thus, an excellent example to demonstrate the importance of the macromolecular engineering to tailor the right material, to open new areas of applications. The PBSA copolyesters family is a nice and promising sustainable material series for some applications such as agriculture, packaging or for some biomedical devices but also for uses where the biodegradation or biocompatibility is not needed such as in automotive or building applications. However, to fulfill the strict requirements of these different fields, some additional tests must be carried out, such as: the study of the biodegradability, biocompatibility, fire retardancy, and specific mechanical and ageing behaviors.

Conflict of interest

The authors declare no conflict of interest.

Acknowledgements

This work has received funding from the European's Union 7th Framework Program for Research, Technological Development and Demonstration under grant agreement n°311815 (SYNPOL Project). In addition, the authors are grateful to the BioAmber company for the supply of Bio-succinic acid. The authors are grateful to Ricardo Pérez-Camargo for his help.

Appendix A. Supplementary material

Supplementary data associated with this article can be found, in the online version, at http://dx.doi.org/10.1016/j.eurpolymj.2016.12.012.

References

[1] L. Avérous, Biodegradable multiphase systems based on plasticized starch: a review, J. Macromol. Sci. Part C: Polym. Rev. 44 (2004) 231–274, http://dx.doi.org/10.1081/MC-200029326.
[2] J. Xu, B.-H. Guo, Poly(butylene succinate) and its copolymers: Research, development and industrialization, Biotechnol. J. 5 (2010) 1149–1163, http://dx.doi.org/10.1002/biot.201000136.
[3] E. Pollet, L. Avérous, Production, chemistry and properties of polyhydroxyalkanoates, in: D. Plackett (Ed.), Biopolym. – New Mater. Sustain. Films Coat, John Wiley & Sons, Ltd., 2011, pp. 65–86. <http://onlinelibrary.wiley.com/doi/10.1002/9781119994312.ch4/summary> (accessed February 16, 2016).
[4] J.J. Bozell, G.R. Petersen, Technology development for the production of biobased products from biorefinery carbohydrates—the US Department of Energy's "Top 10" revisited, Green Chem. 12 (2010) 539, http://dx.doi.org/10.1039/b922014c.
[5] J. Becker, A. Lange, J. Fabarius, C. Wittmann, Top value platform chemicals: bio-based production of organic acids, Curr. Opin. Biotechnol. 36 (2015) 168–175, http://dx.doi.org/10.1016/j.copbio.2015.08.022.
[6] T.A. Werpy, J.E. Holladay, J.F. White, Top Value Added Chemicals from Biomass: I. Results of Screening for Potential Candidates from Sugars and Synthesis Gas, Pacific Northwest National Laboratory (PNNL), Richland, WA (US), 2004. <https://www.osti.gov/scitech/biblio/926125-top-value-added-chemicals-from-biomass-results-screening-potential-candidates-from-sugars-synthesis-gas> (accessed March 23, 2016).
[7] I. Bechthold, K. Bretz, S. Kabasci, R. Kopitzky, A. Springer, Succinic acid: a new platform chemical for biobased polymers from renewable resources, Chem. Eng. Technol. 31 (2008) 647–654, http://dx.doi.org/10.1002/ceat.200800063.
[8] S. Choi, C.W. Song, J.H. Shin, S.Y. Lee, Biorefineries for the production of top building block chemicals and their derivatives, Metab. Eng. 28 (2015) 223–239, http://dx.doi.org/10.1016/j.ymben.2014.12.007.
[9] N.R. Barton, A.P. Burgard, M.J. Burk, J.S. Crater, R.E. Osterhout, P. Pharkya, B.A. Steer, J. Sun, J.D. Trawick, S.J.V. Dien, T.H. Yang, H. Yim, An integrated biotechnology platform for developing sustainable chemical processes, J. Ind. Microbiol. Biotechnol. 42 (2014) 349–360, http://dx.doi.org/10.1007/s10295-014-1541-1.
[10] M. Reulier, L. Avérous, Elaboration, morphology and properties of renewable thermoplastics blends, based on polyamide and polyurethane synthesized from dimer fatty acids, Eur. Polym. J. 67 (2015) 418–427, http://dx.doi.org/10.1016/j.eurpolymj.2014.11.036.
[11] C. Bueno-Ferrer, E. Hablot, M.delC. Garrigós, S. Bocchini, L. Averous, A. Jiménez, Relationship between morphology, properties and degradation parameters of novative biobased thermoplastic polyurethanes obtained from dimer fatty acids, Polym. Degrad. Stab. 97 (2012) 1964–1969, http://dx.doi.org/10.1016/j.polymdegradstab.2012.03.002.
[12] T. Debuissy, E. Pollet, L. Avérous, Synthesis of potentially biobased copolyesters based on adipic acid and butanediols: kinetic study between 1,4- and 2,3-butanediol and their influence on crystallization and thermal properties, Polymer 99 (2016) 204–213, http://dx.doi.org/10.1016/j.polymer.2016.07.022.
[13] L. Avérous, C. Fringant, Association between plasticized starch and polyesters: processing and performances of injected biodegradable systems, Polym. Eng. Sci. 41 (2001) 727–734, http://dx.doi.org/10.1002/pen.10768.
[14] T. Polen, M. Spelberg, M. Bott, Toward biotechnological production of adipic acid and precursors from biorenewables, J. Biotechnol. 167 (2013) 75–84, http://dx.doi.org/10.1016/j.jbiotec.2012.07.008.
[15] D.R. Vardon, M.A. Franden, C.W. Johnson, E.M. Karp, M.T. Guarnieri, J.G. Linger, M.J. Salm, T.J. Strathmann, G.T. Beckham, Adipic acid production from lignin, Energy Environ. Sci. 8 (2015) 617–628, http://dx.doi.org/10.1039/C4EE03230F.
[16] S. Picataggio, T. Rohrer, K. Deanda, D. Lanning, R. Reynolds, J. Mielenz, L.D. Eirich, Metabolic engineering of candida tropicalis for the production of long-chain dicarboxylic acids, Nat. Biotechnol. 10 (1992) 894–898, http://dx.doi.org/10.1038/nbt0892-894.
[17] Y. Tokiwa, B.P. Calabia, C.U. Ugwu, S. Aiba, Biodegradability of plastics, Int. J. Mol. Sci. 10 (2009) 3722–3742, http://dx.doi.org/10.3390/ijms10093722.
[18] E. Takiyama, T. Fujimaki, Biodegradable plastics and polymers, in: Y. Doi, K. Fukuda (Eds.), Biodegrad. Plast. Polym., Elsevier Science, Burlington, 1994, p. 150. <http://public.eblib.com/choice/publicfullrecord.aspx?p=1822412> (accessed October 5, 2016).
[19] M. Ren, J. Song, C. Song, H. Zhang, X. Sun, Q. Chen, H. Zhang, Z. Mo, Crystallization kinetics and morphology of poly(butylene succinate-co-adipate), J. Polym. Sci., Part B: Polym. Phys. 43 (2005) 3231–3241, http://dx.doi.org/10.1002/polb.20539.
[20] B.D. Ahn, S.H. Kim, Y.H. Kim, J.S. Yang, Synthesis and characterization of the biodegradable copolymers from succinic acid and adipic acid with 1,4-butanediol, J. Appl. Polym. Sci. 82 (2001) 2808–2826, http://dx.doi.org/10.1002/app.2135.
[21] M.S. Nikolic, J. Djonlagic, Synthesis and characterization of biodegradable poly(butylene succinate-co-butylene adipate)s, Polym. Degrad. Stab. 74 (2001) 263–270, http://dx.doi.org/10.1016/S0141-3910(01)00156-2.
[22] V. Tserki, P. Matzinos, E. Pavlidou, D. Vachliotis, C. Panayiotou, Biodegradable aliphatic polyesters. Part I. Properties and biodegradation of poly (butylene succinate-co-butylene adipate), Polym. Degrad. Stab. 91 (2006) 367–376, http://dx.doi.org/10.1016/j.polymdegradstab.2005.04.035.
[23] G. Montaudo, P. Rizzarelli, Synthesis and enzymatic degradation of aliphatic copolyesters, Polym. Degrad. Stab. 70 (2000) 305–314, http://dx.doi.org/10.1016/S0141-3910(00)00139-7.
[24] V. Tserki, P. Matzinos, E. Pavlidou, C. Panayiotou, Biodegradable aliphatic polyesters. Part II. Synthesis and characterization of chain extended poly (butylene succinate-co-butylene adipate), Polym. Degrad. Stab. 91 (2006) 377–384, http://dx.doi.org/10.1016/j.polymdegradstab.2005.04.036.
[25] N. Jacquel, F. Freyermouth, F. Fenouillot, A. Rousseau, J.P. Pascault, P. Fuertes, R. Saint-Loup, Synthesis and properties of poly(butylene succinate): efficiency of different transesterification catalysts, J. Polym. Sci. Part A: Polym. Chem. 49 (2011) 5301–5312, http://dx.doi.org/10.1002/pola.25009.
[26] A. Spyros, D.S. Argyropoulos, R.H. Marchessault, A study of poly(hydroxyalkanoate)s by quantitative 31P NMR spectroscopy: molecular weight and chain cleavage, Macromolecules 30 (1997) 327–329, http://dx.doi.org/10.1021/ma9601979.
[27] M. Siotto, L. Zoia, M. Tosin, F. Degli Innocenti, M. Orlandi, V. Mezzanotte, Monitoring biodegradation of poly(butylene sebacate) by gel permeation chromatography, 1H NMR and 31P NMR techniques, J. Environ. Manage. 116 (2013) 27–35, http://dx.doi.org/10.1016/j.jenvman.2012.11.043.
[28] E. Makay-Bödi, I. Vancso-Szercsanyi, Kinetic studies on the polycondensation effects of chain-lengths of the reagents on the reaction rate, Eur. Polym. J. 5 (1969) 145.
[29] I. Vancsó-Szmercsányi, K. Maros-Gréger, E. Makay-Bödi, Investigations on polyesterification reactions, Eur. Polym. J. 5 (1969) 155–161, http://dx.doi.org/10.1016/0014-3057(69)90113-X.
[30] C.-T. Kuo, S.-A. Chen, Kinetics of polyesterification: adipic acid with ethylene glycol, 1,4-butanediol, and 1,6-hexanediol, J. Polym. Sci. Part A: Polym. Chem. 27 (1989) 2793–2803, http://dx.doi.org/10.1002/pola.1989.080270823.
[31] C.C. Lin, K.H. Hsieh, The kinetics of polyesterification. I. Adipic acid and ethylene glycol, J. Appl. Polym. Sci. 21 (1977) 2711–2719, http://dx.doi.org/10.1002/app.1977.070211012.
[32] C.-H. Chen, J.-S. Peng, M. Chen, H.-Y. Lu, C.-J. Tsai, C.-S. Yang, Synthesis and characterization of poly(butylene succinate) and its copolyesters containing minor amounts of propylene succinate, Colloid Polym. Sci. 288 (2010) 731–738, http://dx.doi.org/10.1007/s00396-010-2187-9.
[33] P. Korntner, I. Sumerskii, M. Bacher, T. Rosenau, A. Potthast, Characterization of technical lignins by NMR spectroscopy: optimization of functional group analysis by 31P NMR spectroscopy, Holzforschung 69 (2015) 807–814, http://dx.doi.org/10.1515/hf-2014-0281.
[34] T. Yashiro, H.R. Kricheldorf, S. Huijser, Syntheses of polyesters from succinic anhydride and various diols catalyzed by metal triflates, Macromol. Chem. Phys. 210 (2009) 1607–1616, http://dx.doi.org/10.1002/macp.200900189.
[35] Q. Charlier, E. Girard, F. Freyermouth, M. Vandesteene, N. Jacquel, C. Ladavière, A. Rousseau, F. Fenouillot, Solution viscosity – molar mass relationships for poly(butylene succinate) and discussion on molar mass analysis, Express Polym. Lett. 9 (2015) 424–434, http://dx.doi.org/10.3144/expresspolymlett.2015.41.
[36] K. Chrissafis, K.M. Paraskevopoulos, D.N. Bikiaris, Effect of molecular weight on thermal degradation mechanism of the biodegradable polyester poly (ethylene succinate), Thermochim. Acta 440 (2006) 166–175, http://dx.doi.org/10.1016/j.tca.2005.11.002.

[37] O. Persenaire, M. Alexandre, P. Degée, P. Dubois, Mechanisms and kinetics of thermal degradation of poly(ε-caprolactone), Biomacromolecules 2 (2001) 288–294, http://dx.doi.org/10.1021/bm0056310.
[38] D.N. Bikiaris, K. Chrissafis, K.M. Paraskevopoulos, K.S. Triantafyllidis, E.V. Antonakou, Investigation of thermal degradation mechanism of an aliphatic polyester using pyrolysis–gas chromatography–mass spectrometry and a kinetic study of the effect of the amount of polymerisation catalyst, Polym. Degrad. Stab. 92 (2007) 525–536, http://dx.doi.org/10.1016/j.polymdegradstab.2007.01.022.
[39] T. Zorba, K. Chrissafis, K.M. Paraskevopoulos, D.N. Bikiaris, Synthesis, characterization and thermal degradation mechanism of three poly(alkylene adipate)s: comparative study, Polym. Degrad. Stab. 92 (2007) 222–230, http://dx.doi.org/10.1016/j.polymdegradstab.2006.11.009.
[40] B. Plage, H.R. Schulten, Thermal degradation and mass-spectrometric fragmentation processes of polyesters studied by time/temperature-resolved pyrolysis-field ionization mass spectrometry, Macromolecules 23 (1990) 2642–2648, http://dx.doi.org/10.1021/ma00212a008.
[41] P. Pan, Y. Inoue, Polymorphism and isomorphism in biodegradable polyesters, Prog. Polym. Sci. 34 (2009) 605–640, http://dx.doi.org/10.1016/j.progpolymsci.2009.01.003.
[42] Z. Gan, H. Abe, Y. Doi, Temperature-induced polymorphic crystals of poly(butylene adipate), Macromol. Chem. Phys. 203 (2002) 2369–2374, http://dx.doi.org/10.1002/macp.200290007.
[43] T. Fox, Influence of diluent and of copolymer composition on the glass temperature of a polymer system, Bull. Am. Phys. Soc. 1 (1956) 123–132.
[44] M. Gordon, J.S. Taylor, Ideal copolymers and the second-order transitions of synthetic rubbers. I. Non-crystalline copolymers, J. Appl. Chem. 2 (2007) 493–500, http://dx.doi.org/10.1002/jctb.5010020901.
[45] E. Penzel, J. Rieger, H.A. Schneider, The glass transition temperature of random copolymers: 1, Exp. Data Gordon-Taylor Eq. Polym. 38 (1997) 325–337, http://dx.doi.org/10.1016/S0032-3861(96)00521-6.
[46] F. Chivrac, E. Pollet, L. Avérous, Nonisothermal crystallization behavior of poly(butylene adipate-co-terephthalate)/clay nano-biocomposites, J. Polym. Sci., Part B: Polym. Phys. 45 (2007) 1503–1510, http://dx.doi.org/10.1002/polb.21129.
[47] I. Arandia, A. Mugica, M. Zubitur, A. Arbe, G. Liu, D. Wang, R. Mincheva, P. Dubois, A.J. Müller, How composition determines the properties of isodimorphic poly(butylene succinate-ran-butylene azelate) random biobased copolymers: from single to double crystalline random copolymers, Macromolecules 48 (2015) 43–57, http://dx.doi.org/10.1021/ma5023567.
[48] A. Díaz, L. Franco, J. Puiggalí, Study on the crystallization of poly(butylene azelate-co-butylene succinate) copolymers, Thermochim. Acta 575 (2014) 45–54, http://dx.doi.org/10.1016/j.tca.2013.10.013.
[49] D.W. Van Krevelen, Chapter 5 - calorimetric properties, in: Prop. Polym. Third Complet. Revis. Ed., Elsevier, Amsterdam, 1997, pp. 109–127.
[50] G.Z. Papageorgiou, D.N. Bikiaris, Crystallization and melting behavior of three biodegradable poly(alkylene succinates), Comp. Study Polym. 46 (2005) 12081–12092, http://dx.doi.org/10.1016/j.polymer.2005.10.073.